Entangled photon pair generation in hybrid superconductor–semiconductor quantum dot devices

M. Khoshnegar[1,2] and A. H. Majedi[1,2,3]

[1]*Institute for Quantum Computing, University of Waterloo, Waterloo, Ontario, Canada N2L 3G1*

[2]*Department of Electrical and Computer Engineering, University of Waterloo, Waterloo, Ontario, Canada N2L 3G1*

[3]*Department of Physics and Astronomy, University of Waterloo, Waterloo, Ontario, Canada N2L 3G1*

(Received 27 April 2011; revised manuscript received 9 June 2011; published 8 September 2011)

We investigate the effect of Cooper pair injection in shifting the biexciton energy level of low-symmetry (C_{2v}) quantum dots (QDs) exhibiting nontrivial fine structure splitting. Coupling QDs to the superconducting coherent state forms extra fine structures by intermixing the ground and biexcitonic states where spectroscopic separation of neutral exciton and biexciton can be diminished, yielding a system to be utilized in the time reordering scheme. The separability of exciton and biexciton energy levels is ascribed to the corresponding direct, exchange, and correlation energies calculated here through the configuration interaction method. We demonstrate the possibility of enhancing photon entanglement concurrence via providing an energy coincidence for biexciton-exciton ($XX \rightarrow X$) and exciton-ground ($X \rightarrow 0$) emissions within the weak coupling regime.

DOI: 10.1103/PhysRevB.84.104504 PACS number(s): 78.67.Hc

I. INTRODUCTION

On-demand sources of entangled photons are one of the fundamental building blocks for quantum computing purposes, quantum cryptography, and quantum communication.[1,2] In this context, the biexciton-exciton cascade recombination process in semiconductor QDs has already been proposed for generating polarized-entangled photons.[3] However, the intrinsic fine-structure splitting particularly exhibited by self-organized QDs, owing to predominant long-range electron-hole exchange interaction,[4] degrades the indistinguishability between decay paths and, hence, entanglement of emitted twin photons. Since this exchange interaction is a direct consequence of lateral anisotropy in electron-hole localizations, it can be vanished via symmetrizing the QD carrier confinement[5] or manipulating strain and, hence, the built-in piezoelectric fields.[6] Several methods have been exploited to suppress the destructive effect of fine structure splitting (FSS), including perturbation-induced approaches like the dc and ac Stark effects,[7] magnetic field Zeeman effect,[8] and cavity coupling,[9] or postgrowth techniques, such as thermal[10] and laser[11] local annealing, in order to restore group symmetries equal to C_{4v} or D_{2d}.[12] An alternative route is growing III-V nanowire-QDs along [001] or [111] crystallographic orientation to principally prevent the atomistic asymmetries distorting QD confinement.[13] Furthermore, the so-called "which path" information can be erased through spectral filtering approaches,[14] or the destructive phase developed as a consequence of FSS can be compensated yielding higher fidelities.[15]

One recently proposed method removing any substantial restriction on bright-state splitting (BS) is the time reordering scheme,[16] which demands for biexciton binding energy,

$$\delta_{\mathrm{bi}} = E^{X_1} + E^{X_2} - E^{XX}, \tag{1}$$

to be zero [see Fig. 1(a)]. In this equation, δ_{bi} stands for the biexciton binding energy, E^{X_1} and E^{X_2} are the energies of intermediate excitonic states, and E^{XX} refers to the energy of the biexciton level. Figure 1(a) shows the diagram of the biexciton-exciton cascade process in a typical QD, where δ_{bi} is responsible for energy spacing between biexcitonic and excitonic transitions, and δ_{bs} represents bright-state splitting. The ideal level arrangement for the time reordering scheme is, however, illustrated in Fig. 1(b), having the biexciton energy level tuned equal to the sum of the bright-state energies. Accordingly, the first photon in each path is polarized-entangled to the second photon in the other path having identical energies. In this framework, QD structural properties, including material and geometrical parameters as well as strain field can be manipulated in order to erase δ_{bi} either for binding or antibinding biexcitons.[17] As a result, the carriers' direct and exchange Coulomb interactions slightly vary inside the QD and give rise to a nominal shift in excitonic levels. Practically, this method requires a precise control over QD dimensions and carrier confinement. An alternative solution is to exert lateral electric fields to manage the interplay between single-particle Coulomb interactions and shift the biexciton level upward or downward.

Here, we propose applying a trivial perturbation to the original few-particle states by coupling the QD into the coherent state of a low-band-gap material, such as a superconductor. From the macroscopic point of view, the proximity effect adjacent to the QD region diminishes the superconductor intrinsic gap Δ and, therefore, is capable of providing an energy adjustment ranging from QD's BS (<150 μeV) to biexciton binding energy (a few meVs). In contrast to the previously mentioned methods, here the biexcitonic level is displaced while fourfold excitonic fine structure essentially remains isolated of any change.

This paper is organized as follows. In Sec. II, we describe the intermixing between the QD excitonic states as a consequence of being coupled to the superconductor coherent state. In Sec. III, we briefly explain how the Coulomb interactions in an exemplary QD are calculated. The full description of theoretical modelings can be found in the references addressed within the text. We emphasize that the method of calculation is quite general and could be applied to any QD of the same type. In Sec. IV, we explain the possibility of regulating the newly induced fine structure under external voltage bias. In Sec. V,

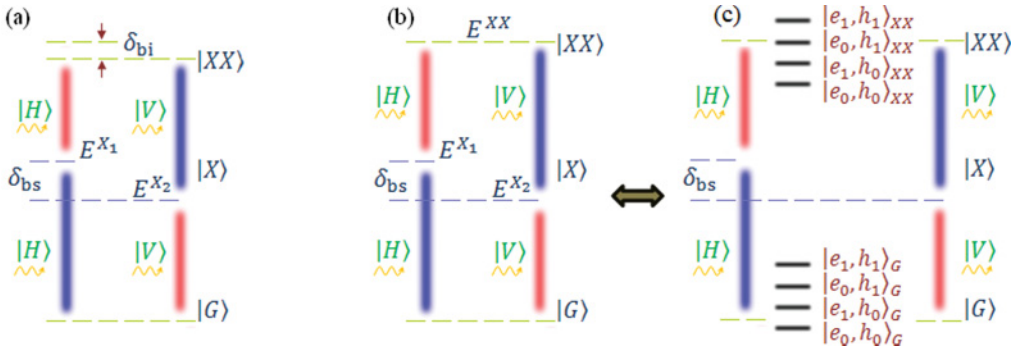

FIG. 1. (Color online) (a) Biexciton-exciton cascade recombination process emitting two photons with identical rectilinear polarization, but dissimilar energies within each path ($|H\rangle$ and $|V\rangle$ stand for photon polarization states in linear representation). Here, δ_{bs} and δ_{bi} denote the bright-state splitting and biexciton binding energy of QD, respectively. (b) In the time reordering scheme where δ_{bi} is removed, photons having orthogonal (for circular polarization: parallel) polarization states are entangled so that properly erase the "which path" information. (c) Cascade recombination in perturbed QD coupled to superconducting leads. QD ground state biexcitonic singlet is split into four levels as a result of being coupled to the BCS coherent state. Depending on the Cooper pair tunneling ratio through QD island, four levels redshift or blueshift and become closely degenerate under special circumstances, eventually developing a new tunable fine structure.

the approximate concurrence of entanglement is calculated, and in Sec. VI, a summary of our results is provided.

II. INTERMIXING OF QD STATES

Hybrid superconductor-QD devices have already been realized presenting Cooper pair tunneling through QD in three different regimes.[18] Defining Γ as the level broadening of the successive tunneling intermediate state, J as the average Coulomb interaction of single particles, and Δ as the superconducting intrinsic gap, these regimes are categorized as: (1) strong coupling ($\Gamma \gg J$, $\Gamma \gg \Delta$), in which the negligible Coulomb blockade cannot prohibit the Cooper pair tunneling of electrons and holes, thus supercurrent can flow through the device analogous to the single-particle current; (2) intermediate coupling, where the energy scales are in the same range, i.e. $\Gamma \sim J$, $\Gamma \sim \Delta$. $\Gamma \sim J$ indicates that coupling is adequate so that considerable supercurrent appears even when the Fermi level of leads and QD energy levels are off resonance. Furthermore, $\Gamma \sim \Delta$ ensures that, under Fermi level alignment, a significant supercurrent can flow even in the presence of high Coulomb interactions; (3) weak coupling ($\Gamma \ll J$, $\Gamma \ll \Delta$): in the limit of weak coupling, the resonant tunneling of Cooper pairs is predominantly prohibited by Coulomb blockade giving rise to, for example, quasiparticle fourth-order cotunneling mechanisms; however, the device still exhibits Josephson junction behavior with critical current $I_c \sim (2e/\hbar)\Gamma^2/\Delta$.[19] Nevertheless, supercurrent can transfer through the QD via higher-order quantum coherent tunneling processes.[20] The effective Hamiltonian of the superconductor-coupled QD for the isolated electrons (neglecting the presence of hole particles) reads[21,22]

$$\hat{\mathcal{H}}_e = \sum_{\sigma_e} E_e \hat{c}^\dagger_{\sigma_e}\hat{c}_{\sigma_e} + J_{ee}\hat{n}_\uparrow\hat{n}_\downarrow + \tilde{\Delta}_e\hat{c}^\dagger_\uparrow\hat{c}^\dagger_\downarrow + \tilde{\Delta}^*_e\hat{c}_\uparrow\hat{c}_\downarrow, \qquad (2)$$

where $\hat{c}^\dagger_{\sigma_e}(\hat{c}_{\sigma_e})$ creates (annihilates) an electron possessing spin $\sigma_e \in \{1/2, -1/2\}$, and $\hat{n}_{\sigma_e}$ stands for the number operator of the same particle. Here, E_e and J_{ee} are the single electron kinetic energy and electron-electron on-site Coulomb repulsion, respectively. The collective motion of Cooper pairs experiences a suppression of superconductivity when approaching the QD, known as proximity effect, where the intrinsic gap begins to diminish and an effective superconducting gap $\tilde{\Delta}_e$ is defined. Here, $\tilde{\Delta}_e$ depends on the Coulombic interactions and level broadening, thus needs to be renormalized when QD energy levels change.[20] An exactly analogous Hamiltonian governs the dynamics of isolated holes, and Eq. (2) is valid when energies are redefined for hole particles and $\hat{c}^\dagger_{\sigma_e}$, $\hat{c}_{\sigma_e}$, and $\hat{n}_{\sigma_e}$ are replaced with $\hat{h}_{\sigma_h}$, $\hat{h}^\dagger_{\sigma_h}$, and $\hat{n}_{\sigma_h}$. The only difference lies in the pseudospin of holes: valence subbands of III–V materials in zinc blende or wurtzite phase are categorized into three families near Γ_8 or Γ_7 valleys, including heavy-hole (HH), light-hole (LH) and spin-orbit split-off (SO). Depending on the position of the QD level in the energy space, it has contribution from all these subbands with different weights as a consequence of band mixing. However, the predominant contribution to the valence band (VB) ground state (the topmost energy level) comes from the HH band, where the z projection of total angular momentum or equivalently the hole's pseudospin is $\sigma_h \in \{3/2, -3/2\}$. The second contribution associated with the closest LH band is trivial, especially when the QD height is small and vertical confinement becomes strong.

In order to determine the realistic energy levels of the coupled electron-hole system, their direct and exchange Coulomb interactions must be considered. Diagonalizing the Hamiltonian in Eq. (2) leads to one unperturbed doublet having energies $\xi_{\uparrow D} = \xi_{\downarrow D} = \xi_D$ (hereinafter, energies are indicated with respect to the superconductor chemical potential, i.e. $\xi_D = E_e - \mu^e$), and two singlets with energies $\xi_{S_0,S_1} = \xi_D + J_{ee}/2 \pm [(\xi_D + J_{ee}/2)^2 + |\tilde{\Delta}_e|^2]^{1/2}$ being mixed of the ground and one-pair excited states:[21]

$$|e_{0;e}\rangle_S = -e^{-i\varphi_e}|u_e||G_e\rangle + |v_e||\Theta_e\rangle, \qquad (3a)$$

$$|e_{1;e}\rangle_S = e^{-i\varphi_e}|v_e||G_e\rangle + |u_e||\Theta_e\rangle. \qquad (3b)$$

where $|G_e\rangle$ corresponds to BCS ground state, and $|\Theta_e\rangle$ represents the situation where one Cooper pair of electrons

is transferred into the QD ($|\Theta_e\rangle = \hat{c}^\dagger_\uparrow \hat{c}^\dagger_\downarrow |G_e\rangle$); v_e and u_e are coherence factors denoting the probability of a state being occupied by Cooper pairs $|v_e|^2$ or quasiparticles $|u_e|^2$.[23] Here, φ_e stands for the superconducting condensate phase, and subscript S ascribes these eigenfunctions to singlet mixed states. The doublet is the bare QD single particle state experiencing no energy variation under the above circumstance; however, it gives rise to the possible odd parity cycles and is of importance when trionic optical transitions, X^+ and X^- are included in the model.[21,24] These odd cycles seem to be a principal issue in the weak coupling limit where the number of quasiparticles entering the QD is sizable in comparison with Cooper pairs: in the case that quasiparticle tunneling is the superior injection mechanism, negatively X^- or positively X^+ charged excitons are expected to inevitably contribute to the spectrum, although their spectral sharp-lines can be filtered out. Nevertheless, to simplify the model, we neglect odd cycles in this work. A similar treatment is applicable to the hole side again by replacing $|G_h\rangle$ and $|\Theta_h\rangle$ in Eq. (2), where $|\Theta_h\rangle = \hat{h}^\dagger_\uparrow \hat{h}^\dagger_\downarrow |G_h\rangle$. Expanding the total Hamiltonian

$$\hat{\mathcal{H}}_{\rm tot} = \hat{\mathcal{H}}_e + \hat{\mathcal{H}}_h + \sum_{eh} J^{d,ex,{\rm corr}} \hat{n}_e \hat{n}_h \tag{4}$$

on mixed subspace $\{|e\rangle \otimes |h\rangle\} = \{|e_0,h_0\rangle,|e_1,h_0\rangle,|e_0,h_1\rangle,|e_1,h_1\rangle\}$, i.e. $\mathcal{H}_{mn} = \langle h,e|_n \mathcal{H}_{\rm tot}|e,h\rangle_m$, induces fourfold fine structures in the vicinity of both ground and biexcitonic states. This induced fine structure is schematically illustrated in Fig. 1(c). In the expression above, J^d, J^{ex}, and $J^{\rm corr}$ are the QD ground state direct, exchange, and correlation energies. The energy regulation of extra sublevels then depends on two parameters: chemical potential of the leads μ_l, and the tunneling rate which is already preserved in $\tilde{\Delta}$ (we assume that the superconducting effective gap is equal for both electron and hole sides). It is convenient to go to the number state representation by performing a unitary transformation τ with matrix elements depending on μ_l, $\tilde{\Delta}$, and superconducting phase $\varphi_{e,h}$, i.e. $\{|G_e,G_h\rangle,|\Theta_e,G_h\rangle,|G_e,\Theta_h\rangle,|\Theta_e,\Theta_h\rangle\} = \tau(v_{e,h},u_{e,h},\phi_{e,h})\{|e\rangle \otimes |h\rangle\}$. As the QD bright states are essentially fixed, $|G_e, G_h\rangle$ and $|\Theta_e, \Theta_h\rangle$ energy levels can be finely tuned to effectively remove the biexciton binding energy. Henceforth, we label the energy of the four induced states as follows: $E_0 = E_{|e_0,h_0\rangle}$, $E_1 = E_{|e_1,h_0\rangle}$, $E_2 = E_{|e_0,h_1\rangle}$, and $E_3 = E_{|e_1,h_1\rangle}$.

III. QD FEW-PARTICLE INTERACTIONS

Here, we explain the proposed method by giving a relevant specific example. The approach of calculations given here, consisting of the $k.p$ model and configuration interaction (CI) method, is, however, quite general for III–V materials in zinc blende phase.[25] In the case where the QD emitter is made of wurtzite-structured material, the appropriate single-particle $k.p$ Hamiltonian must be replaced.[25] Necessity of calculating the on-site Coulomb interactions relies on these facts: first, it confirms the ordering of Γ, J, and Δ, thus the regime of device operation. Secondly, it is a commonly used experimental method to tune the QD energy levels and also its electron and hole Coulomb interactions by applying an appropriate gate voltage. This gate voltage induces an electric field mostly along the lateral directions of the QD, thus separating electron and hole probability densities leading to lower electron-hole interactions, together with a reduction in excitonic oscillator strength, which is not favorable in photon emission applications. However, as long as the oscillator strength is not drastically suppressed, gate manipulation is a practical solution for tuning the Coulombic interactions of the QD. In the following, we show that for conventional QDs working as single photon sources in the infrared wavelength range, the Coulombic interactions are adequately large that energy ordering of Γ, J, and Δ dictates the device operation to be in the weak coupling regime.

Our setup consists of a typical single self-assembled InAs/GaAs quantum dot grown along [001] direction on top of a 2-ML InAs wetting layer capped by GaAs as the local barrier and connected laterally to superconducting electrodes.[19] The biexciton binding energy, which is defined with respect to the recombination energy of the exciton ground state, $\delta_{\rm bi} = \hbar\omega_{|X\rangle_D \to |G\rangle_D} - \hbar\omega_{|XX\rangle_D \to |X\rangle_D}$, reads[26]

$$\begin{aligned}\delta_{\rm bi} = &-2J^d_{eh} - J^d_{ee} - J^d_{hh} + 2J^{\rm corr}_{|X\rangle_{\rm D}} \\ &- J^{\rm corr}_{|XX\rangle_{\rm D}} + 2J^{ex}_{|X\rangle_{\rm D}} - J^{ex}_{|XX\rangle_{\rm D}},\end{aligned} \tag{5}$$

where subscript D stands for the excitonic levels of a bare dot. The direct terms, J^d_{ee}, J^d_{hh}, and J^d_{eh}, along with exchange terms, $J^{ex}_{|X\rangle_D}$ and $J^{ex}_{|XX\rangle_D}$, contributing to the expression above are primarily determined by taking only wave functions of QD ground state into account: the single particle wave functions of carriers trapped inside the QD is composed of two components, the Bloch spinor and its associated envelope function. For instance, in the simplest case, the total wave function of an electron in the S orbital of a conduction band (CB) can be represented by $\psi^e_{\sigma_{e_0}} = \phi^e_0 |S_{CB};\sigma_{e_0}\rangle$, and similarly the total wave function of a hole in the P orbital of a valence heavy-hole band is given by $\psi^h_{\sigma_{h_0}} = \phi^h_0 |P_{HH};\sigma_{h_0}\rangle$. However, there are some coupling coefficients between the conduction and valence wave functions, included in the $k.p$ model, originating from the QD asymmetries. These coupling terms are also responsible for the nonzero long-range exchange interaction which gives rise to the splitting of bright states. As long as the QD confinement maintains laterally symmetric, the coupling remains trivial. On the other hand, as mentioned above, the QD valence ground state is usually an admixture of HH and LH bands, commonly with larger weight from the HH part. The mixing coefficient between these two subbands depends on the QD geometry, especially its vertical anisotropy: the large amount of anisotropy in the vertical orientation (growth direction) of the QD leads to higher mixing orders between HH and LH. Consequently, nearly flat QDs keep the VB ground state relatively HH-type in character. Figure 2(c) shows the density of Coulomb interaction matrix elements[4]

$$\rho_{p_0q_0,\sigma\sigma'} = \psi^{q_0}_{\sigma'_{q_0}} {}^* \psi^{p_0}_{\sigma'_{p_0}} {}^* C(\mathbf{r}_1,\mathbf{r}_2) \psi^{p_0}_{\sigma_{p_0}} \psi^{q_0}_{\sigma_{q_0}} \tag{6a}$$

$$\mathcal{H}^{|X\rangle_{\rm D}}_{p_0q_0;\sigma\sigma'} = \left\langle \psi^{p_0}_{\sigma'_{p_0}} \psi^{q_0}_{\sigma'_{q_0}} \middle| C(\mathbf{r}_1,\mathbf{r}_2) \middle| \psi^{p_0}_{\sigma_{p_0}} \psi^{q_0}_{\sigma_{q_0}} \right\rangle, \tag{6b}$$

where $C(\mathbf{r_1},\mathbf{r_2}) = e^2/4\pi\varepsilon(\mathbf{r_1},\mathbf{r_2})|\mathbf{r_1} - \mathbf{r_2}|$. Here, $p_0,q_0 \epsilon \{e_0,h_0\}$ represent particle labels dwelling in the ground states, and ε denotes the static dielectric constant. The corresponding direct interactions can be then evaluated as

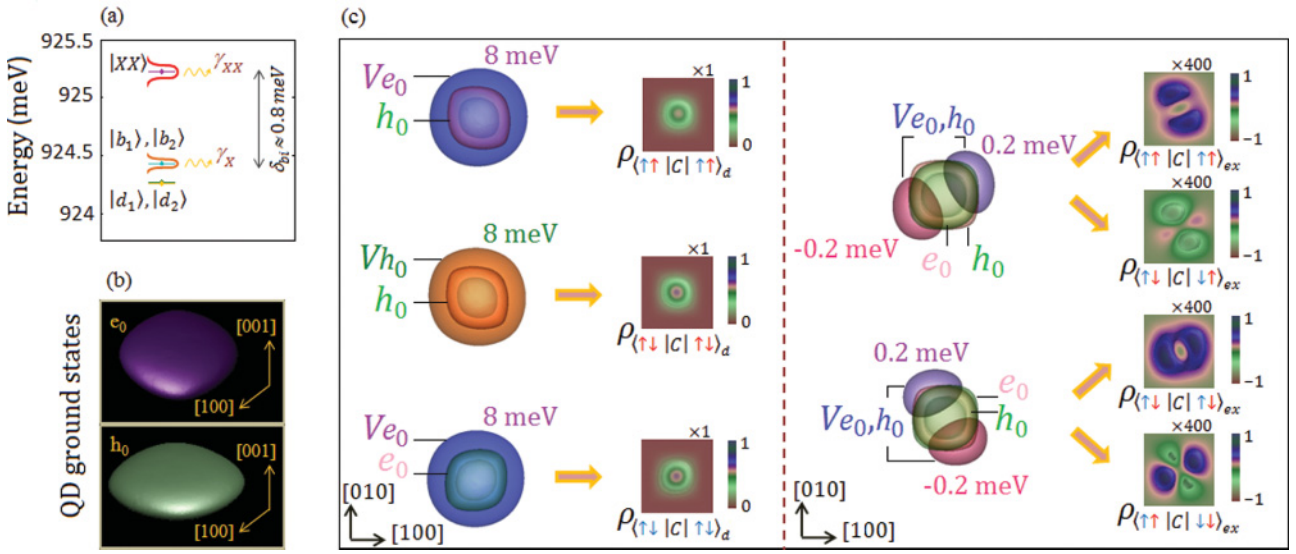

FIG. 2. (Color online) (a) Biexciton $|XX\rangle$ and exciton, bright $|b_1\rangle$, $|b_2\rangle$ and dark $|d_1\rangle$, $|d_2\rangle$ singlets, energy levels of a 25-nm long, 5-nm high [001]-oriented InAs/GaAs truncated pyramidal QD on a 2 ML InAs wetting layer before being coupled to superconducting leads. Biexciton is antibinding with $\delta_{\rm bi} \approx -0.8$ meV. (b) Electron and hole ground state probability densities, e_0 and h_0, slightly extended along [110] and [1$\bar{1}$0] directions as a consequence of the existing piezoelectric polarization. QD flatness minimizes heavy-hole (HH) and light-hole (LH) intermixing giving rise to significant isolation of the first HH band. As a result, the most contribution to h_0 probability density is attributed to HH envelope function. (c) Left panel: direct Coulomb interactions, J_{ee}, J_{hh}, and J_{eh}, can be obtained by locating the charge density of one single particle in the mean-field potential caused by the other single particle. Here, V_{e0} and V_{h0} are the electron- and hole-induced potentials, and e_0 and h_0 label electron and hole probability densities. The normalized density of the CI matrix elements, $\rho_{p_0q_0,\sigma\sigma'}$, for the ground state direct interaction terms are plotted on (001) plane 1 nm above the QD base. Each $\psi^{p|q}_{\sigma|\sigma'}$ in Eq. (6) is symbolized by its associated spin and color: the electron spin and the z projection of hole total angular momentum are distinguished by blue and red arrows, respectively. Subscript d stands for the normalized density of direct matrix element. Right up panel: exchange interaction terms calculated by putting the electron-hole mixed charge densities $\psi^{e}_{\uparrow_e}{}^{*}\psi^{h}_{\uparrow_h}$ or $\psi^{e}_{\downarrow_e}{}^{*}\psi^{h}_{\downarrow_h}$ in the potential, V_{e_0,h_0}, formed by the other mixed charge density $\psi^{e}_{\uparrow_e}{}^{*}\psi^{h}_{\uparrow_h}$. Right down panel: exchange interaction terms when the electron-hole mixed charge densities $\psi^{e}_{\downarrow_e}{}^{*}\psi^{h}_{\uparrow_h}$ or $\psi^{e}_{\uparrow_e}{}^{*}\psi^{h}_{\downarrow_h}$ are located inside the potential formed by the other mixed charge density $\psi^{e}_{\uparrow_e}{}^{*}\psi^{h}_{\downarrow_h}$. Subscript ex means the normalized density of exchange matrix element, which is 400 times scaled up for the sake of clarity. Only real parts are illustrated for $\langle\uparrow_e\uparrow_h|C|\downarrow_e\downarrow_h\rangle_{ex}$ and $\langle\uparrow_e\downarrow_h|C|\downarrow_e\uparrow_h\rangle_{ex}$.

$J^{d}_{p_0,q_0} = \langle\psi^{p_0}_{\sigma'}\psi^{q_0}_{\sigma'}|C|\psi^{p_0}_{\sigma}\psi^{q_0}_{\sigma}\rangle$, where $\sigma\sigma' = \uparrow\downarrow$ if $p_0 = q_0$, otherwise $\sigma\sigma' = \uparrow\uparrow$. Analogously, the ground-state exchange terms $J^{ex}_{p_0,q_0}$, which originate the bright- and dark-state splittings, are calculated by replacing $|\psi^{p_0}_{\sigma}(\mathbf{r}_1)\psi^{q_0}_{\sigma}(\mathbf{r}_2)\rangle$ by $|\psi^{p_0}_{\sigma}(\mathbf{r}_2)\psi^{q_0}_{\sigma}(\mathbf{r}_1)\rangle$ in $J^{d}_{p_0,q_0}$. Above single-band treatment, however, only covers the Fermi correlations. To account for the Coulomb correlations arising in many-body systems, higher energy levels shall be regarded: eight-band $k.p$ Hamiltonian[25] was employed to solve for the single-particle wave functions of a 25-nm long in base ($b_D = 25$ nm), 5-nm high ($h_D = 5$ nm) zinc blende InAs/GaAs truncated pyramidal QD. The vertical aspect ratio of $h_D/b_D = 0.2$ provides the required separability between HH and LH bands, hence, the pseudospin of holes in VB ground state is semipurely $\pm$ 3/2. Besides, our calculations show that for this vertical aspect ratio, the electron-electron and hole-hole repulsive interactions are both comparable to electron-hole attractive interaction, yielding less biexciton binding energy. The required material parameters, including $k.p$ parameters and elasticity constants, are taken from Refs. 13 and 23. Provided the single-particle states by $k.p$ method, CI approach was then utilized to construct the true wave function of few-particle multiexcitons and calculate the direct and exchange Coulomb interactions along with the correlation energies:[26] 10 hole and eight electron subbands were included to build up the configuration set. The calculated exciton and biexciton energy levels are depicted in Fig. 2(a). The negligible intrinsic BS (<2 μeV) obtained here is a consequence of a laterally symmetric and vertically flat QD.[13] Particularly, the QD flatness suppresses the role of strain-induced piezoelectric polarization,[27] which plays a destructive role on the C_{4v} symmetry of electron- and hole-envelope functions and, hence, the degeneracy of QD bright states. Although the QD studied here is potentially an ideal source of entangled photons due to its small BS, the nondeterministic growth process of QDs giving rise to possible geometrical imperfections puts no guarantee on their lateral symmetry in practice.[5] Therefore, in the present work, we focus on optimally removing the biexciton binding energy, making cascade levels appropriate for time reordering measurements, while the conclusions given in the following are legitimate also for large BS QDs.

From CI calculations, we exploited $J_{eh} = J^{d}_{eh} = -12.54$ meV, $J_{ee} = J^{d}_{ee} = 12.97$ meV, and $J_{hh} = J^{d}_{hh} = 13.2$ meV, much larger than the intrinsic gap Δ of a typical low T_c superconductor, like niobium ($\Delta_{\rm Nb} \approx 1.5$ meV at T = 0). This indicates that: (1) in QDs having almost vertical symmetry, where the electron and hole probability

densities are similarly localized in space, direct Coulomb interactions are comparable and relatively cancel out each other in Eq. (5). The summation of the exchange ($\sum_{|X\rangle_D,|XX\rangle_D} J^{ex} \leqslant \Delta$) and correlation ($\sum_{|X\rangle_D,|XX\rangle_D} J^{\text{corr}}$) energies then significantly participate in δ_{bi} determination. (2) Having $\tilde{\Delta}_{e,h} = \Gamma_{e,h} \exp(i\varphi_{e,h})/2$,[28] the condition $J^d > \Delta$ ensures that the device operates in the weak coupling regime and $|G_e, G_h\rangle$ is the equilibrium quasistate since the probability of being in quasistate $|\Theta_e, \Theta_h\rangle$ is given by $|\tilde{\Delta}_{e,h}|^4/J^{d4} \ll 1$ in second-order perturbation.[22] Hereinafter, we assume that the chances of electrons passing into and escaping from the QD states are equal, i.e. $\Gamma = \Gamma_e = \Gamma_h$. This presumption is valid until the device is symmetric and simplifies the model without loss of generality.

IV. MIXED STATES FINE TUNING

In order to activate the recombination process, quasistate $|\Theta_e, \Theta_h\rangle$ must be pumped up by imposing a bias voltage into the leads to separate their chemical potentials, μ_l^e and μ_l^h, close to the QD excitonic band gap. Meanwhile, by adjusting the detuning $\Delta\varepsilon_{e,h}$, defined as the energy spacing between chemical potentials and single-particle energy levels, E_e and E_h, $|G_e, G_h\rangle$ and $|\Theta_e, \Theta_h\rangle$ quasistates tend toward a selected degeneracy point.[22] Sequential injection of Cooper pairs of electrons (holes) then fills up the intermediate $|\Theta_e, G_h\rangle$($|G_e, \Theta_h\rangle$) and finally $|\Theta_e, \Theta_h\rangle$ quasistates. Subsequently, $|\Theta_e, \Theta_h\rangle$ decays radiatively into the ground state $|G_e, G_h\rangle$ through intermediate excitonic bright states and closes the cycle by emitting polarized photons.

One technique to directly reduce $|G_e, G_h\rangle$ and $|\Theta_e, \Theta_h\rangle$ energy level splitting δ_s is controlling over chemical potential detuning, under the situation where $J_{ee}, J_{hh}, J_{eh} \gg \Delta$ and $\sum_{|X\rangle_D,|XX\rangle_D} J^{\text{corr}} + J^{ex} \lesseqgtr \Delta$. The latter condition is evidently determined by the type of superconductor and also the geometry of the QD. For instance, the calculations given by A. Schliwa *et al.* in Ref. 26 demonstrate that the biexciton correlation energy can even reach half of the direct interaction energies for large vertical aspect ratios. These calculations also confirm that both exciton and biexciton correlation energies are minimized for the vertical aspect ratio we have chosen in our example (0.2). Our calculations exhibit an acceptable consistency with their results in terms of the evolution of exciton and biexciton correlation energies versus vertical aspect ratio. In our case, the correlation terms were estimated <2 meV, depending on the number of basis regarded for the configuration space.

We spanned detuning over the energy range $-J_{eh}^{XX}$ to J_{eh}^{XX}, the largest energy scale among Coulomb interactions ($J_{eh}^{XX} = 4J_{eh}$, since the total electron-hole interaction for the biexciton is established between the four constituting single particles of two excitons, and the change of spin configurations between these excitons does not affect the direct interactions), and plotted the eigenfunctions of the hybrid system fine structure. The informative part of the plot is shown in Figs. 3(a) and 3(b): the approximate hopping energy for electron (hole) is presumed to be $J_{ee}^d/2$ ($J_{hh}^d/2$) without loss of generality. Then by setting $\Delta\varepsilon_{e0} = J_{eh}^{XX}/2 + J_{ee}/2$ and $\Delta\varepsilon_{h0} = -J_{eh}^{XX}/2 + J_{hh}/2$, the quasistates $|G_e, G_h\rangle$, $|\Theta_e, G_h\rangle$, and $|\Theta_e, \Theta_h\rangle$, or their equivalent mixed states, reside nearby at one specific degeneracy point [see anticrossing in Fig. 3(a)]. At the immediate vicinity of anticrossing, which never vanishes as long as the superconducting gap exists, mixed states have contribution from all above quasistates. Along the skew narrow region, the induced ground $|G\rangle$ and biexciton $|XX\rangle$ states can be estimated through $|G\rangle \approx \alpha_1|G_e, G_h\rangle + \beta_1|\Theta_e, \Theta_h\rangle$ and $|XX\rangle \approx \alpha_2|G_e, G_h\rangle + \beta_2|\Theta_e, \Theta_h\rangle$. Instead, $|G\rangle$ mixed state becomes a combination of $|G_e, G_h\rangle$ and $|\Theta_e, G_h\rangle$ adjacent to the vertical narrow region, and finally turns into a pure state elsewhere. Figs. 3(a) and 3(b) depict α_i and β_i, $i = \{1, 2\}$, coefficients of the ground and biexciton states for $\Gamma = 0.5\Delta$ and 1.5Δ, where Δ is assumed to be equal to the superconducting gap of niobium at T = 0, $\Delta \approx \Delta_{\text{Nb}} = 1.52$ meV. Changing the level broadening Γ over the range $\sim 0.1\Delta$ to $\sim 3\Delta$ reproduces the same patterns shown here, but the Γ value always regulates the gap opened at anticrossing. Moving along the skew region, which is shown to be the approximate degeneracy area of $|G_e, G_h\rangle$ and $|\Theta_e, \Theta_h\rangle$ quasistates in Fig. 3(c), toward anticrossing, β_i decreases, giving rise to a transition into $|G_e, G_h\rangle$ state. For initiating the sequential carrier-tunneling photon-generation cycle, we need to set the operational point very close to the anticrossing, where $|G_e, G_h\rangle$, $|\Theta_e, \Theta_h\rangle$, and their intermediate level $|\Theta_e, G_h\rangle$ come to degeneracy. We name the respective detunings leading to this degeneracy as $\Delta\varepsilon_{e0}$ and $\Delta\varepsilon_{h0}$. Such an initialization is clarified in Fig. 3(c) for $\Gamma = 0.5\Delta_{\text{Al}}$, where we replaced niobium with aluminum in our model to acquire higher energy precision appropriate for fine-tuning the splitting δ_s ($\Delta_{\text{Al}} \sim 165\ \mu\text{eV} \sim 0.1\Delta_{\text{Nb}}$ at T = 0): the bold blue area shows the regions where the difference between ground and biexciton energy levels, E_3 and E_0, is less than Δ_{Al}. Analogously, the pale blue area specifies where the ground and $|\Theta_e, G_h\rangle$ intermediate quasistates separate less than Δ_{Al}.

Although μ_l^e and μ_l^h could be modified to shift $\delta_s = E_3 - E_0$ over a relatively large range, i.e. at least in the order of Δ, they might not be able to explicitly minimize this splitting for a certain value of $\tilde{\Delta}$. We set detunings $\Delta\varepsilon_e$ and $\Delta\varepsilon_h$ on the skew curve $\Gamma = 0.5\Delta_{\text{Al}}$, about $5\tilde{\Delta} = 1.25\Delta_{\text{Al}}$ away from the exact degeneracy point yielding to $\sim 15\ \mu$eV splitting. According to the expected BS exhibited by self-assembled QDs ($20-100\ \mu$eV),[8,29] such a splitting energy implies no advantage of the time reordering scheme over the regular polarized-entangled photon generation method.[3] This brings us to the conclusion that, although chemical potentials can provide a wide-sweep range for biexciton binding energy, an effective suppression in δ_s and, hence, required energy resolution for entanglement purposes might not necessarily occur.

V. TUNNELING RATIO AND CONCURRENCE

The tunneling ratio of Cooper pairs suggests an extra degree of freedom to the above system since it directly determines the level broadening $\Gamma(E) = \Sigma_m |q_m|^2 \delta(E_m - E)$,[20] where q_m is the transmission probability to the mth QD energy level. The underlying concept would be then similar to pushing the system to an alternative skew region near the fixed anticrossing point ($\Delta\varepsilon_{e0}$, $\Delta\varepsilon_{h0}$). Figures 3(d) and 3(e) describe how δ_s variations might be connected to Γ in the weak coupling limit (if we call the level broadening at which the energy spacing between E_3 and E_0 is minimized as critical

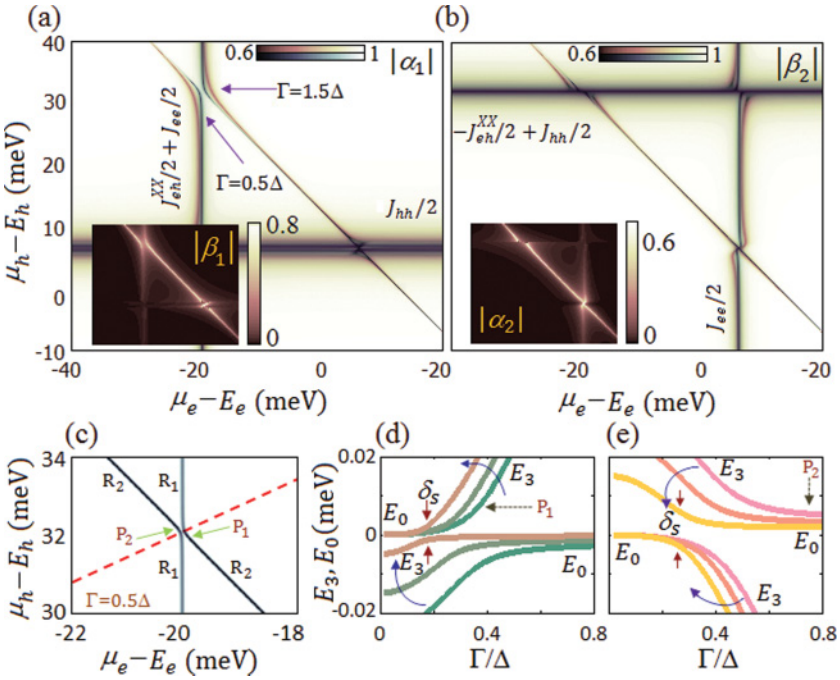

FIG. 3. (Color online) (a) and (b) $|\alpha_i|$ and $|\beta_i|$ coefficients of the coupled system ground $|G\rangle$ and biexcitonic $|XX\rangle$ states against detunings $\Delta\varepsilon_e$ and $\Delta\varepsilon_h$ for $\Gamma = 0.5\Delta_{\rm Nb}$ and $1.5\Delta_{\rm Nb}$. Sweep window only includes areas near the anticrossing for the sake of clarity. As demonstrated, along the skew region, $|G_e, G_h\rangle$ and $|\Theta_e, \Theta_h\rangle$ components contribute dominantly to $|G\rangle$ and $|XX\rangle$ wave functions. (c) $\Gamma = 0.5\Delta_{\rm Al}$, bold blue branch R_2 shows the regions where $\delta_s < \Delta_{\rm Al} \sim 0.16$ meV: $|G\rangle$ and $|XX\rangle$ are almost degenerate. Pale blue branch R_1 shows the regions where $|G\rangle$ and $|e_1, h_0\rangle = \alpha_3|G_e, G_h\rangle + \beta_3|\Theta_e, G_h\rangle$ become degenerate ($\delta_{|G\rangle,|e_1,h_0\rangle} < \Delta_{\rm Al}$). Dashed red line passes exactly through the anticrossing. P_1 and P_2 are selected points on the skew branch separated 200 μeV from anticrossing. The last two plots illustrate the ground and biexciton energy levels varying versus level broadening. Chemical potential of the electron side μ_l^e is changed in 5 μeV steps starting from (d) P_1 and (e) P_2 toward anticrossing while the hole side chemical potential μ_l^h is kept fixed.

Γ labeled by Γ_c, then the conditions $\Gamma_c \approx 0.2\Delta, 0.25\Delta$, and $\Gamma_c \ll J^d_{ee}, J^d_{hh}, J^d_{eh}$ confirm the operation in the weak coupling regime), and manifests the capability of δ_s to be reduced below radiative linewidth of exciton in typical self-assembled QDs (e.g. $\sim$4 μeV).[29,30] In these two plots, we first set the chemical potentials on P_1 and P_2, then minimize δ_s at some point by smoothly fluctuating one of the chemical potentials, here μ_l^e, around the initial point and sweeping over Γ. This mostly happens moving deeper into the weak coupling regime; however, the least probability of pair tunneling must be consistently satisfied.

It is noteworthy to mention that other than the amount of δ_s, the distinguishability of photons generated in each decay path also relies on the bare QD excitonic line widths together with superconducting coherence factors, i.e. ($\hbar = 1$)

$$\mathcal{R}_{|XX\rangle\to|X_\lambda\rangle} = \gamma_{\rm ph}|\beta_2(u_{e,h}, v_{e,h})|^2\gamma_{|\Theta_e,\Theta_h\rangle\to|X_\lambda\rangle} \quad (7a)$$

$$\mathcal{R}_{|X_\lambda\rangle\to|G\rangle} = \gamma_{\rm ph}|\alpha_1(u_{e,h}, v_{e,h})|^2\gamma_{|X_\lambda\rangle\to|G_e,G_h\rangle}, \quad (7b)$$

where $|X_\lambda\rangle$ is the excitonic intermediate state with polarization $\lambda = \{H, V\}$, $\gamma_{\rm ph}$ denotes the photon line width, and the excitonic transition rate reads $\gamma_{|i\rangle\to|f\rangle} = |\langle f||\hat{\mathcal{H}}_{\rm em}|i\rangle|^2$, having

$$\hat{\mathcal{H}}_{\rm em} = \sum_{S;p;\lambda} g^S_{p\lambda}\hat{a}^\dagger_{p\lambda}\hat{b}_\lambda + {\rm H.c.} \quad (8)$$

In above equation, $S = \{|\Theta_e,\Theta_h\rangle \to |X_{H,V}\rangle, |X_{H,V}\rangle \to |G_e,G_h\rangle\}$, $\hat{b}_H = 1/\sqrt{2}(\hat{h}_\downarrow\hat{c}_\uparrow + \hat{h}_\uparrow\hat{c}_\downarrow)$, $\hat{b}_V = i/\sqrt{2}(\hat{h}_\downarrow\hat{c}_\uparrow - \hat{h}_\uparrow\hat{c}_\downarrow)$, $\hat{a}^\dagger_p$ creates a photon in pth optical mode, and g^S_λ incorporates the oscillator strength in each excitonic transition. According to Eqs. (7a) and (7b), since the individual line widths of cross generated photons are affected by $|\alpha_1|$, $|\beta_2|$ factors, the degree of entanglement can be either ruined or improved in our hybrid system. Assuming $\mathcal{R}_{XX} = \mathcal{R}_{|XX\rangle\to|X_V\rangle} = \mathcal{R}_{|XX\rangle\to|X_H\rangle}$ and $\mathcal{R}_X = \mathcal{R}_{|X_H\rangle\to|G\rangle} = \mathcal{R}_{|X_V\rangle\to|G\rangle}$, one can evaluate the concurrence for the generated states of photons as a measure of entanglement:[16]

$$C = \frac{4\zeta_{XX}\zeta_X}{\pi^2}\left|\int \frac{W_{\rm opt}(\omega_m,\omega_n)}{|\omega_m+\omega_n-\omega_{XX}-i\zeta_{XX}|^2(\omega_m-\omega_{|X_H\rangle}+i\zeta_X)(\omega_m-\omega_{|X_V\rangle}+i\zeta_X)}d\omega_m d\omega_n\right|, \quad (9)$$

where ω_{XX} and $\omega_{|X_{\lambda=H,V}\rangle}$ are the biexciton and exciton frequencies, and the spectral half widths of exciton and biexciton are represented by ζ_X and ζ_{XX}: $\zeta_X = \mathcal{R}_X/2\gamma_{\rm ph}$ and $\zeta_{XX} = \mathcal{R}_{XX}/2\gamma_{\rm ph}$. One can simply manipulate the additional phase $W_{\rm opt}$ above in order to enhance the concurrence. The best choice of $W_{\rm opt}$ is still under debate (see papers in Ref. 16); however, in the simplest case one can introduce an optical delay τ_0 to add a linear phase, i.e. $W_{\rm opt} = \exp[i(\omega_m - \omega_n)\tau_0]$. Under the condition where color coincidence between the biexciton and exciton is prepared, τ_0 can be optimized to provide the maximum concurrence. Pathak and Hughs have shown that this time delay only depends on the exciton and biexciton spectral half widths: $\tau_0 = \ln(1 + \zeta_{XX}/2\zeta_X)/\zeta_{XX}$.[16] However, out of the color coincidence condition, this time delay must be altered depending on the biexciton binding energy in order to optimize the concurrence. Generally, two parameters determine the amount of concurrence in the time reordering scheme applied to the biexciton cascade process: (1)

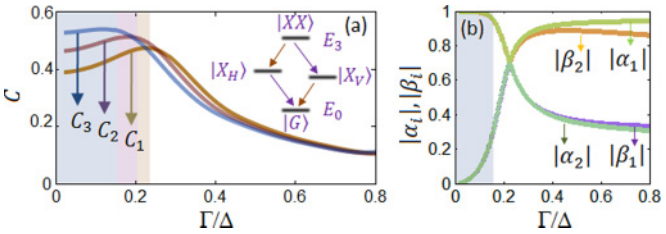

FIG. 4. (Color online) (a) Concurrence defined in Eq. (9) plotted versus level broadening for $\Delta = \Delta_{\mathrm{Al}}$, assuming $\gamma_{|XX\rangle\to|X_V\rangle,|X_H\rangle} = 2\gamma_{|X_V\rangle,|X_H\rangle\to|G\rangle}$ and $\gamma_{|X_V\rangle,|X_H\rangle\to|G\rangle} = 4\mu$eV. In the three curves shown here, C_1, C_2, and C_3, chemical potential on the electron side μ_l^e changes in 2 μeV steps starting from P_2 (curve C_1) toward anticrossing, whereas hole-side chemical potential μ_l^h is held fixed. (b) $|\alpha_i|$ and $|\beta_i|$ coefficients corresponding to curve C_3 from (a). The maximum concurrence does not occur exactly where δ_s is minimized due to the contribution from exciton linewidth ζ_X.

$\delta_b/\zeta_X = (\omega_{XX} - \omega_{|X_H\rangle} - \omega_{|X_V\rangle})/\zeta_X$, where δ_b is the energy separation of the existing biexciton level and the ideal one when the color coincidence of excitonic and biexcitonic transition occurs—in our model, δ_s is a good measure to represent this energy spacing; (2) the ratio between the exciton and biexciton lifetimes, or equivalently their spectral line widths ζ_{XX}/ζ_X. Going back to Eqs. (7a) and (7b), this ratio relies upon α_1 and β_2 in addition to bare QD transition rates, $\gamma_{|\Theta_e,\Theta_h\rangle\to|X_{H,V}\rangle}$ and $\gamma_{|X_{H,V}\rangle\to|G_e,G_e\rangle}$. Near anticrossing shown in Fig. 3(a), where $|\alpha_1|, |\beta_2| < 1$, concurrence C comprises δ_s, α_1, and β_2 information as a consequence of intermixing. This reflects that by tuning $\Delta\varepsilon_e$, $\Delta\varepsilon_h$, and Γ in order to minimize δ_s, the potentially maximum concurrence might not necessarily be achieved. However, by controlling over W_{opt} reaching the optimum limit is feasible when realistic values of excitonic broadenings, $\gamma_{|\Theta_e,\Theta_h\rangle\to|X_\lambda\rangle}$ and $\gamma_{|X_\lambda\rangle\to|G_e,G_h\rangle}$, are known.

We examined the evolution of concurrence C given in Eq. (9) versus Γ in the same sense accomplished for δ_s [see Fig. 4(a)]. We biased the model exactly at P_2 [see Fig. 3(c)] by setting the appropriate chemical potentials μ_l^e and μ_l^h, then changed the level broadening Γ over a relatively large scale (curve C_1). For smaller values of Γ, the concurrence is merely a function of δ_s/ζ_X, since both $|\alpha_1|$ and $|\beta_2|$ are almost equal [see Fig. 4(b)] and the ζ_{XX}/ζ_X ratio remains constant. In contrast, for larger values of Γ, $|\alpha_1|^2/|\beta_2|^2$ is increased as can be deduced from Fig 4(b), giving rise to smaller ζ_{XX}/ζ_X ratios and a local rise in concurrence. We also changed μ_l^e by 2 μeV steps toward anticrossing to show how concurrence might be improved for smaller δ_s values; see curves C_2 and C_3 in Fig 4(a). In Ref. 16, Avron *et al*. demonstrated that for a fixed amount of ζ_{XX}/ζ_X, the concurrence is enhanced when the δ_b/ζ_X approaches zero. However, in our model both δ_s and ζ_X undergo a significant change, moving deeper into the weak coupling regime (e.g. $\Gamma < 0.4\Delta$), where the interplay between their variations leads to a local maximum of concurrence next to the anticrossing.

We note that here the cascade process is presumed to be isolated of cross-dephasing between $|X_H\rangle$ and $|X_V\rangle$, which indeed lowers the concurrence in practice and is a fundamental issue when intermediate exciton states are not identical nor symmetrically coupled.[30] Notice also that throughout the analysis we restricted the operation regime into the weak coupling limit where the hybridization factor $|\tilde{\Delta}|$, as the key property of setup, was represented by $\Gamma/2$, whereas in practice the relative measure of $\tilde{\Delta}$ and Γ is not fully restrained.[21,22] Reminding the fact that the intermixing phenomenon explicitly depends on the effective superconducting gap, there is a possibility to reduce it for the sake of energy resolution without suppressing tunneling probability. A simple procedure for dynamical modification of effective gap might be the application of a small magnetic field which leaves the QD features unaffected. Another option would be exploiting a back gate to manage the charging and, hence, Coulomb interactions inside QD, and eventually impose required changes on Γ and $\tilde{\Delta}$.[31] However, in the latter case, losing a part of oscillator strength seems inevitable.

VI. SUMMARY

In conclusion, by providing a relevant example, we studied the applicability of superconductor-coupled QDs in enhancing the degree of entanglement via suppressing the biexciton binding energy under the time reordering scheme. This method allows for tuning biexciton binding energy over a relatively large energy range, in contrast to the setups utilizing lateral strain[17] or local electric filed,[32] by forming extra fine structures near ground and biexcitonic energy levels and, hence, results in the observation of well-defined entangled photon pair state. The reason is that here the new energy levels commute somehow independent of the QD confinement and its original fine structure, but rather are linked to the characteristics of superconducting contacts such as Δ and Γ. We believe that appropriate contacting of large BS QDs, rendering weak coupling, can optimize the concurrence even in a laser- or cavity-free setup and without requiring any postgrowth manipulation of QDs.

ACKNOWLEDGMENTS

We would thank A. J. Salim and M. Ansari from Quantum Device group at IQC for their fruitful discussions on Cooper pair tunneling through semiconductor QDs.

[1]E. Knill, R. Laflamme, and G. J. Milburn, Nature **409**, 46 (2001); A. Shields, Science **297**, 1821 (2002).

[2]H. J. Briegel, W. Dur, J. I. Cirac, and P. Zoller, Phys. Rev. Lett. **81**, 5932 (1998); T. Jennewein, C. Simon, G. Weihs, H. Weinfurter, and A. Zeilinger, *ibid*. **84**, 4729 (2000).

[3]O. Benson, C. Santori, M. Pelton, and Y. Yamamoto, Phys. Rev. Lett. **84**, 2513 (2000).

[4]Here we utilized Green's formula to decompose the sixfold integral into solving a Poisson's equation and performing a subsequent three-fold integration. See O. Stier, *Electronic and Optical*

Properties of Quantum Dots and Wires, Berlin Studies in Solid State Physics (Wissenschaft und Technik Verlag, Berlin, 2001), Vol. 7.

[5]A. Mohan, M. Felici, P. Gallo, B. Dwir, A. Rudra, J. Faist and E. Kapon, Nature Photonics **4**, 302, (2010).

[6]S. Seidl, M. Kroner, A. Högele, K. Karrai, R. J. Warburton, A. Badolato, and P. M. Petroff, Appl. Phys. Lett. **88**, 203113 (2006).

[7]B. D. Gerardot, S. Seidl, P. A. Dalgarno, R. J. Warburton, D. Granados, J. M. Garcia, K. Kowalik, and O. Krebs, Appl. Phys. Lett. **90**, 041101 (2007); W. A. Coish and J. M. Gambetta, Phys. Rev. B **80**, 241303(R) (2009).

[8]R. M. Stevenson, R. J. Young, P. Atkinson, K. Cooper, D. A. Ritchie, and A. J. Shields, Nature **439**, 179 (2006); R. M. Stevenson, R. J. Young, P. See, D. G. Gevaux, K. Cooper, P. Atkinson, I. Farrer, D. A. Ritchie, and A. J. Shields, Phys. Rev. B **73**, 033306 (2006).

[9]R. Johne, N. A. Gippius, G. Pavlovic, D. D. Solnyshkov, I. A. Shelykh, and G. Malpuech, Phys. Rev. Lett. **100**, 240404 (2008); Y. X. Liu, S. K. Ozdemir, M. Koashi, and N. Imoto, Phys. Rev. A **65**, 042326 (2002); Y. X. Liu, A. Miranowicz, M. Koashi, and N. Imoto, *ibid.* **66**, 062309 (2002).

[10]A. Rastelli, A. Ulhaq, S. Kiravittaya, L. Wang, A. Zrenner, and O. Schmidt, Appl. Phys. Lett. **90**, 073120 (2007).

[11]R. Seguin, A. Schliwa, T. D. Germann, S. Rodt, K. Pötschke, A. Strittmatter, U. W. Pohl, D. Bimberg, M. Winkelnkemper, T. Hammerschmidt, and P. Kratzer, Appl. Phys. Lett. **89**, 263109 (2006).

[12]K. F. Karlsson, M. A. Dupertuis, D. Y. Oberli, E. Pelucchi, A. Rudra, P. O. Holtz, and E. Kapon, Phys. Rev. B **81**, 161307(R) (2010).

[13]R. Singh and G. Bester, Phys. Rev. Lett. **103**, 063601 (2009).

[14]N. Akopian, N. H. Lindner, E. Poem, Y. Berlatzky, J. Avron, D. Gershoni, B. D. Gerardot and P. M. Petroff, Phys. Rev. Lett. **96**, 130501 (2006).

[15]Z. Q. Zhou, C. F. Li, G. Chen, J. S. Tang, Y. Zou, M. Gong, and G. C. Guo, Phys. Rev. A **81**, 064302 (2010).

[16]J. E. Avron, G. Bisker, D. Gershoni, N. H. Lindner, E. A. Meirom and R. J. Warburton, Phys. Rev. Lett. **100**, 120501 (2008); P. K. Pathak and S. Hughes, *ibid.* **103**, 048901 (2009); J. E. Avron, G. Bisker, D. Gershoni, N. H. Lindner, E. A. Meirom and R. J. Warburton, *ibid.* **103**, 048902 (2009).

[17]F. Ding, R. Singh, J. D. Plumhof, T. Zander, V. Křápek, Y. H. Chen, M. Benyoucef, V. Zwiller, K. Dörr, G. Bester, A. Rastelli, and O. G. Schmidt, Phys. Rev. Lett. **104**, 067405 (2010).

[18]G. Katsaros, P. Spathis, M. Stoffel, F. Fournel, M. Mongillo, V. Bouchiat, F. Lefloch, A. Rastelli, O. G. Schmidt, and S. De Franceschi, Nature Nanotechnology **5**, 458 (2010).

[19]S. De Franceschi, L. Kouwenhoven, C. Schönenberger, and W. Wernsdorfer, Nature Nanotechnology **5**, 703 (2010).

[20]J. A. van Dam, Y. V. Nazarov, E. P. A. M. Bakkers, S. De Franceschi, and L. P. Kouwenhoven, Nature **442**, 667 (2006); A. V. Rozhkov, D. P. Arovas, and F. Guinea, Phys. Rev. B **64**, 233301 (2001).

[21]T. Meng and S. Florens, Phys. Rev. B, **79**, 224521 (2009).

[22]F. Hassler, Y. V. Nazarov, and L. P. Kouwenhoven, Nanotechnology **21**, 274004 (2010).

[23]M. Tinkham, *Introduction to Superconductivity* (McGraw-Hill, New York, 1996), p. 56.

[24]O. Gywat, H. J. Krenner, and J. Berezovsky, *Spins in Optically Active Quantum Dots: Concepts and Methods* (Wiley-VCH, Weinheim, 2010), p. 132.

[25]T. B. Bahder, Phys. Rev. B **41**, 11992 (1990); C. Pryor, *ibid.* **57**, 7190 (1998); M. Khoshnegar, M. Sodagar, A. Eftekharian, and S. Khorasani, IEEE. J. Quantum. Electron. **46**, 228 (2010).

[26]A. Schliwa, M. Winkelnkemper, and D. Bimberg, Phys. Rev. B **79**, 075443 (2009).

[27]A. Schliwa, M. Winkelnkemper, and D. Bimberg, Phys. Rev. B **76**, 205324 (2007).

[28]C. W. J. Beenakker and H. van Houten, in *Single-Electron Tunneling and Mesoscopic Devices* (Springer, Berlin, 1992), pp. 175–179.

[29]P. Michler, *Single Semiconductor Quantum Dots* (Springer, Berlin, 2009), p. 236.

[30]A. J. Hudson, R. M. Stevenson, A. J. Bennett, R. J. Young, C. A. Nicoll, P. Atkinson, K. Cooper, D. A. Ritchie, and A. J. Shields, Phys. Rev. Lett. **99**, 266802 (2007); R. M. Stevenson, A. J. Hudson, A. J. Bennett, R. J. Young, C. A. Nicoll, D. A. Ritchie, and A. J. Shields, *ibid.* **101**, 170501 (2008).

[31]M. P. van Kouwen, M. E. Reimer, A. W. Hidma, M. H. M. van Weert, R. E. Algra, E. P. A. M. Bakkers, L. P. Kouwenhoven and V. Zwiller, Nano Lett. **10**, 1817 (2010).

[32]M. E. Reimer, M. Korkusiński, D. Dalacu, J. Lefebvre, J. Lapointe, P. J. Poole, G. C. Aers, W. R. McKinnon, P. Hawrylak, and R. L. Williams, Phys. Rev. B **78**, 195301 (2008).